Use of *Eichhornia Crassipes* as a Bioadsorbent for the Removal of Methyl Orange and Methylene Blue Present in Residual Solutions

Carlos David Hernández-Origel[1], Laura Patiño-Saldivar[1], Mercedes Salazar-Hernández[2], Alba Nelly Ardila[3], Alfonso Talavera-López[4], Rosa Hernánez-Soto[1], José Alfredo Hernández[1*]

[1] UPIIG, del Instituto Politécnico Nacional, Av. Mineral de Valenciana 200, Col. Fraccionamiento Industrial Puerto, 36275 Silao, Guanajuato, Mexico

[2] Departamento de Ingeniería en Minas, Metalurgia y Geología, División de Ingenierías, Universidad de Guanajuato, Ex Hacienda. de San Matias S/N, San Matías, San Javier, 36020 Guanajuato, México

[3] Politécnico Colombiano Jaime Isaza Cadavid, Carrera 48. El Poblado, No.7–151, Código Postal: 4932, Medellín, Colombia

[4] Ciencias Químicas, Universidad de Zacatecas, Campus UAZ siglo XXI, Carretera Zacatecas–Guadalajara Km. 6, Col. Ejido "La Escondida", C.P. 98160, Zacatecas, México

* Corresponding author's e-mail: jahrnandezma@ipn.mx

ABSTRACT

The textile industry is very important because its products are widely used by society, however, this activity has a great contribution to the contamination of water resources due to its effluents that contain large amounts of colorants, among which is the blue of methylene (MB) and methyl orange (MO) that can cause damage to the health of living being. For this reason the present study concerned the removal of these dyes by adsorption using *Eichhornia Crassipes* (Water lily) with different treatments. The results show that the chemisorption removal process using two sites per dye molecule having an exothermic nature for the water-treated lily and for the NaOH-treated lily is endothermic. The maximum adsorption capacities of 228.9 mg/g for MB (60 °C) and 155.38 mg/g (30 °C) for MO with the NaOH treatment were achieved. The SEM analysis shows that there are significant changes in the surface due to the treatments. The XRD patterns indicate that with the pretreatment with NaOH the crystallinity of WL increases while the treatment with water maintains the presence of amorphous cellulose. In the FTIR spectra, the bands corresponding to different functional groups such as lignin, cellulose and hemicellulose that participate in the adsorption of both dyes are observed.

Keywords: bioadsorbents; equilibrium; freundlich, kinetic; water lily.

INTRODUCTION

In recent years there has been a great damage to the ecological balance mainly due to anthropogenic activities such as urbanization, industrialization and due to the rapid increase of these operations making it very difficult to care for the environment [Uddin et al., 2021; Zhang et al., 2019]. It is known that the industrial and agricultural sector consume more than 90% of the water available to living beings [Marquez et al., 2021; Rashid et al., 2019] with which large amounts of wastewater

are produced, around 50% of wich are discharged into the public sewer causing damage to health [Marquez et al., 2021; Rashid et al., 2019]. Industries such as cosmetics, food, biomedicine, paper, and textiles use dyes to produce their products generating around 10 thousand tons/year of waste [Uddin et al., 2021; Amalraj et al., 2021; Kadhom et al., 2020]. This has caused several problems due to toxicity, low biodegradation on the entire ecosystem around this discharge of the dyes due to their direct interference in the photosynthesis process, in addition to causing various diseases to

humans in the skin and respiratory system [Panneerselvam et al., 2021; Marquez et al., 2021; Amalraj et al., 2021; Bożęcka et al., 2021]. Dyes are divided into anionic (acid dyes), nonionic (dispersed) and cationic (basic dyes), among them are methyl orange (MO) and methylene blue (MB) which have a similar molecular mass [Kadhom et al., 2020; Lacin et al., 2020; Uddin et al. 2021]. MB is a cationic dye used in different products as chemical, medical, and biological applications its chemical structure makes it difficult to remove [Amalraj et al., 2021; Bożęcka et al., 2021; Kadhom et al., 2020] and MO is an anionic dye that is used for dyeing and due to its poor biochemical purification it is very difficult to degrade [Zhang et al., 2019; Amalraj et al., 2021; Bożęcka et al., 2021]. Several methods have been proposed for the removal of various dyes: physicochemical (filtration, osmosis, dialysis, etc.), biological, chemical (oxidation, precipitation, photocatalysis, etc.), although the latter, despite being quite efficient, are not used widely due to their high demand for chemical substances, and electrical energy, which makes these chemical methods very expensive [Saini et al., 2020; Zhang et al., 2019; Deng et al., 2020; Kadhom et al. 2020]. Among the proposed methods, adsorption stands out, as it is a viable process due to its simple operation, easy regeneration, low cost and high efficiency in the treatment of wastewater containing dyes [Uddin et al., 2021; Márquez et al., 2021; Bożęcka et al., 2021].

There are conventional adsorbents such as clays, zeolites, low-cost and high-abundance mesoporous materials, however, the search for new materials that have a similar adsorption capacity and a high removal percentage has been carried out in recent decades [Lacin et al., 2020; Márquez et al., 2021; Amalraj et al., 2021], The agro-industrial waste have a very low cost such as peanut shells, wheat, tamarind, rice, orange, egg, walnut, etc., have been shown to have a removal capacity very similar to conventional adsorbents for the elimination of heavy metals, dyes, etc.[Saini et al., 2020; Zhang et al., 2019; Kadhom et al., 2020]. On the other hand, plants have also been usedfor elimination of dyes, such as Nymphaea alba (white nymph), Nymphaea nucifera (Sacred lotus) [Kalam et al., 2021; Rashid et al., 2019; Sharma et al., 2021; Pratel S. et al. 2012], Pistia stratrioes (Water lettuce) and Oesdogonium obtaining good results used for the bioadsorption of dyes found in the effluents the textile industry [Rashid et al., 2019; Tabinda et al., 2019; Panneerselvam et al., 2021].

Within the management of plants for the adsorption process, one that has attracted attention is the Water Lily (*Eichhornia crassipes*), wich is a freshwater plant that floats freely in rivers, lakes, a lagoon that has high available due to its rapid growth and its great adaptability to many ecosystems, causing it to become an invasive species since it increases the evapotranspiration process and, interferes with human activities causing economic losses [Priya et al., 2017; Tabinda et al., 2019; Panneerselvam et al., 2021]. Several strategies (chemical and biological) have been used to eliminate the weed but it is very difficult to eradicate, since its seeds remain feasible for a long period of time [Patel S. 2012; Tabinda et al., 2019; Panneerselvam et al., 2021]. On the other hand, the feasibility of taking advantage of this biomass for the processing of wastewater has recently been studied using biodsorption for the treatment of the effluent with heavy metals such as Cr, Pb, Cu, etc.. It was very effective, removing up to 90% of these pollutats and it is a reusable biomaterial, since it can last several adsorption cycles [Patel S. 2012; Panneerselvam et al., 2021]. In the removal process of various dyes, good results have been obtained when *E. crassipes* was treated with inorganic salts [Tsade-Kara et al., 2021], obtaining biochar [Prassad et al., 2021], EDTA [Acosta-Rodríguez et al., 2021], among other compounds, achieving a comparable adsorption capacity with commercial adsorbents. On the basis of this , it has been decided to study the use of *E. crassipes* extracted from the Yuriria lagoon, Guanajuato in Mexico, as bioadsorbent in the removal of MB and MO analyzing the effect of the modification of the surface with water and NaOH, the effect of the parameters that affect of the adsorption of dyes (temperature, contact time, initial concentration of dyes, adsorbent concentration) in the removal process of MB and MO to determine the adsorption mechanism of both dyes b characterizing the biomaterial before and after the reaction of the dyes as well as using different isotherm and kinetic models.

MATERIALS AND METHODS

Reagents

All reagents used were analytical grade. The water used for all the solutions prepared in the experimentation was deionized. The used dyes,

methylene blue (MB, $\lambda_{max} = 665$ nm) and methyl orange (MO, $\lambda_{max} = 465$ nm) of Meyer Chemistry, were used without any additional purification [Joaquin-Medina et al., 2021].

Preparation and treatment of water lily

The water lily (WL) from Lake Yuriria, Guanajuato, Mexico was washed with running water at room temperature, dried in a forced convection oven (Shel Lab CE5F) at 80 °C for 24 h and it was crushed with an industrial blender (Tapisa Acero Inoxidable) until a fine powder (100 mesh) was obtained, for subsequent pretreatment. The water lily was subjected to a treatment with deionized water (WLW) with a ratio of 30 g/L (P/V) at 75 °C and constant stirring for 1 h for its subsequent filtration with a vacuum pump (Thomas 1CZC8). This process was repeated until obtaining a crystalline filtrate. WL was treated with sodium hydroxide (NaOH), at 0.5 M (WLN) with a ratio of 30 g/L (P/V) and had an initial pH of 13.65, stirred for 2 h at 60 °C. Subsequently, it was filtered and the solid was mixed with a 1 M HCl solution (pH ~1) while stirring for 1 h at room temperature. After this time the solid was filtered and washed with 10 times the amount of water used in the HCl solution, finally drying the solid at 85 °C overnight in a forced convection oven. With this treatment, for every 100 g of plant, 81.5 g of a WL powder is obtained at a cost of $7 and $13 for the treatment with water and methanol, respectively.

Equilibrium dye removal (adsorption isotherms)

For the equilibrium study of the adsorption of the dyes, a mass ratio of adsorbent/volume of solution of 0.5 g/L was used and the concentration was varied from 0 to 50 ppm of MB and from 0 to 40 ppm MO, were shaken in a shaker (ZH-WY-200D) at 200 rpm at 30, 45 and 60 °C until equilibrium is reached (~11 h of contact time). The samples were centrifuged (Generic 6-TRPR) at 6000 rpm for 10 min. They were analyzed to determine the concentration of the different dyes present in the solution by UV-Vis spectrophotometry (VELAB VE-5000). The amount of dye removed by adsorbent, q, was obtained with the following expression [Joaquin-Medina et al., 2021; Patiño-Saldivar et al., 2021]:

$$q = \frac{V(C_0 - C)}{m} \quad (1)$$

where: C_0 and C – the initial concentration and in equilibrium (mg/L);
V – the volume of solution (L);
m – the mass of WL (g).

The removal percentage, %R, was calculated as follows [Joaquin-Medina et al. 2021; Patiño-Saldivar et al., 2021]:

$$\%R = \frac{(C_0 - C)}{C_0} * 100 \quad (2)$$

The different models of isotherms are shown in Table 1.

The regression coefficient was calculated to evaluate the fit of each nonlinear model and the separation factor, R_L, which allows predicting the affinity between the adsorbent and adsorbate, using the following equation [Joaquin-Medina et al. 2021; Patiño-Saldivar et al., 2021]:

$$R_L = \frac{1}{1 + K_L C_0} \quad (3)$$

where: K_L – the constant of the Langmuir model,
C_0 – the initial concentration of MB and MO.

Table 1. Non-linear adsorption isotherm models [Joaquin-Medina et al. 2021]

Model	Equation	Description
Langmuir	$q_e = \dfrac{q_m K_L C_e}{1 + K_L C_e}$	q_m, is the maximum adsorbed capacity (mg/g); K_L (L/mg) is the constant of the Langmuir model that is related to the separation factor (R_L); K_S (L/mg) is the slaving Sips model constant related to adsorption energy and β is the constant of the Sips model; K_F [(mg/g)(L/mg)]$^{1/n}$ is the Freundlich constant related to adsorption capacity and 1/n indicates adsorption energy; K_{DR} (mol/J)^2 is the speed constant; ε (J/mol) is the parameter of the DR model $\varepsilon = RT\ln\left(1 + \dfrac{1}{C_e}\right)$; E is the energy required to remove a dye molecule from the solution. $E = \dfrac{1}{\sqrt{2k_{DR}}}$
Freundlich	$q_e = K_F C_e^{\frac{1}{n}}$	
Dubinin-Radushkevich (DR)	$q_e = q_m exp(-k_{DR}\varepsilon^2)$	
Sips	$q_e = \dfrac{q_m(K_s C_e)^\beta}{1 + (K_s C_e)^\beta}$	

To understand the thermodynamics of the adsorption process, thermodynamic parameters such as apparent Gibbs free energy were determined:

$$\Delta G = -RT ln(55.5 K_L) \qquad (4)$$

where: K_L – the constant of the Langmuir (L/mol) model);
  R – the ideal gas constant;
  T – the absolute temperature (K).

$$ln(55.5 K_L) = \frac{\Delta S}{R} - \frac{\Delta H}{RT} \qquad (5)$$

The values of ΔH and ΔS can be determined with the slope and sorted to the origin of the ΔG chart as a function of $1/T$.

Batch dye removal (adsorption kinetics)

The adsorption kinetics were performed using MB 25 ppm solutions and for MO is 20 ppm, the adsorbent concentration was varied from 1 to 5 g/L, shaking in a shaker at 200 rpm at 30, 45 and 60 °C, with a contact time of 9 h, taking an aliquot every 1.5 h, which was centrifuged at 6000 rpm for 10 min. They were analyzed to know the concentration of the different dyes present in the solution by UV-Vis spectrophotometry. Experimental data were adjusted with the adsorption kinetics models found in Table 2.

In addition to using the coefficient of determination to compare the efficiency of the different kinetic and equilibrium models, the standard deviation, Δq%, was calculated [21]:

$$\Delta q\% = 100 * \sqrt{\frac{\left(\frac{q_{exp} - q_{cal}}{q_{exp}}\right)^2}{N - 1}} \qquad (6)$$

where: N is the number of data,
  q_{exp} and q_{cal} (mg/g) are the experimental and calculated values of the removed dyes, respectively.

Characterization of bioadsorbents

Attenuated total reflectance-fourier transform spectroscopy (ATR-FTIR) analyses before and after adsorption of DNS were carried out over the wave number range of 4000–400 cm⁻¹ using a Thermo Scientific Nicolet iS10 analyzer, 32 scans were obtained with a resolution of 4 cm⁻¹. X-ray diffraction patterns (XRD) were obtained in a diffractometer (Ultima IV Rigaku). To determine the isoelectric point, a sample of adsorbent in water with an initial ratio of 0.05 g was stirred at 200 rpm for 24 h. in 50 mL to determine its pH with a potentiometer (Science Med SM-25CW): 0.05 g was added every 24 h until the pH did not change.

RESULTS AND DISCUSSION

Equilibrium adsorption study of MO and MB with WL

The knowledge about the interaction between the dyes and WL could be obtained by analyzing the adsorption data in the equilibrium, adjusting them to the isotherm models described in Table 1. In Figure 1, the data obtained at different temperatures for the removal of MB (Figure 1a) and MO (Figure 1b) where it can be noted that the adsorption of MB and MO decreases as the temperature increases, which indicates that the treatment with water allows the reduction of the concentration of the dyes to be favored at low temperatures. In the same figure the different settings of the isotherm models to the experimental data can be observed, to obtain the parameters and thus know the adsorption mechanism of each dye shown in Table 3 where the deterministic coefficient criteria (R^2) and the normalized standard deviation (Δq%) for choosing the best fit between the different models.

On the basis of the established criteria, it was determined that the Freundlich model for

Table 2. Models of adsorption isotherm used for the analysis of experimental data [Patiño-Saldivar et al., 2021; Joaquin-Medina et al. 2021]

Model	Equation	Description
Pseudo first order (PPO)	$q = q_{max}[1 - exp(-k_1 t)]$	q_t, adsorption capacity (mg/g); C_o is the initial concentration of the dye in the liquid (mg/L); V (L) is the volume of the dye solution and m (g), is the mass of the adsorbent; q_{max}, is the maximum adsorbed capacity (mg/g); k_1 (1/h) is the speed constant of the PPO model; k_2 (g s/mg) is the speed constant of the PSP model; α is the initial rate of adsorption (mg/g h); β is the constant of the Elovich model related to the surface area covered and the activation energy by chemisorption (mg/g).
Pseudosecond order (PSO)	$q = \dfrac{t}{\dfrac{1}{k_2 * q_{max}^2} + \dfrac{t}{q_{max}}}$	
Elovich	$q = \dfrac{1}{\beta}[ln(t) + ln(\alpha * \beta)]$	

both dyes regardless of temperature, which indicates that the surface is highly heterogeneous, and that the adsorption of the dye molecules can be carried out in more than one layer

on the surface of WL and this removal process is chemically [Kalam et al., 2021, Azam et al., 2020; Prasad et al., 2021]. On the other hand, the separation factor (R_L) showed that its value
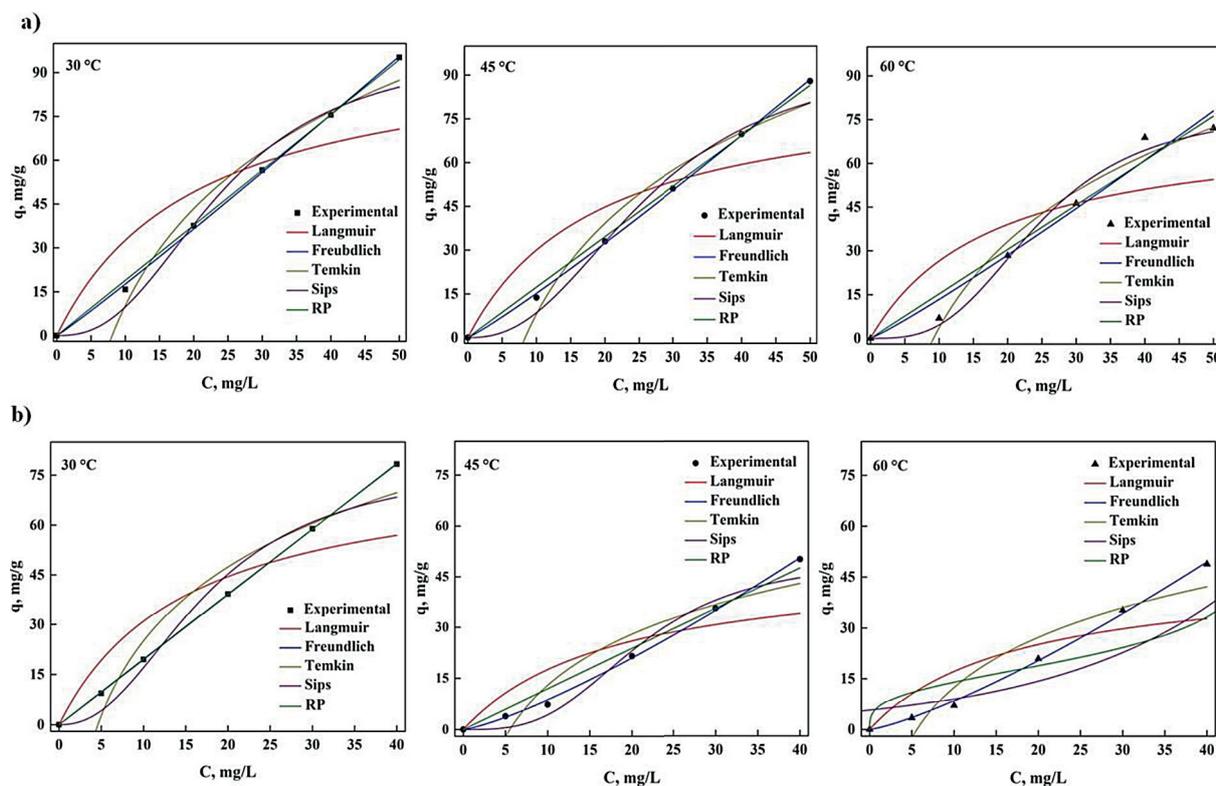

Figure 1. Equilibrium data for dye adsorption using WLW: a) MB and b) MO

Table 3. Parameters of the isotherm models in the adsorption of MB and MO with WLW

Models	Parameter	MB			MO		
		T			T		
		30°C	45°C	60°C	30°C	45°C	60°C
Langmuir	K_L	0.086	0.0611	0.046	0.0740	0.0574	0.044
	q_m	98.01	88.73	69.58	48.11	47.04	60.04
	R_L	0.7–0.23	0.77–0.29	0.81–0.35	0.73–0.25	0.77–0.3	0.82–0.36
	R^2	0.827	0.789	0.708	0.739	0.759	0.789
	Δq, %	13.75	1.669	13.28	152.7	14.12	71.85
Freundlich*	K_F	1.571	1.217	0.955	0.699	0.765	1.017
	n	0.952	0.913	0.902	0.781	0.802	0.955
	R^2	0.999	0.999	0.997	0.999	0.999	0.999
	Δq, %	1.787	1.001	4.687	1.415	0.253	0.961
SIPS	K_S	0.041	0.037	0.041	0.047	0.048	0.057
	q_m	98.74	90.88	78.75	50.75	48.75	78.75
	n_S	2.506	2.393	3.097	3.161	3.309	2.292
	R^2	0.973	0.981	0.989	0.971	0.972	0.963
	Δq, %	16.25	13.86	34.99	139.3	37.69	191.6
DR	q_m	88.15	100.0	105.4	62.94	61.533	80.48
	k_{DR}	78.66	80.76	73.38	71.07	61.09	71.01
	E, J/mol	79.73	80.68	82.55	82.75	83.87	119.4
	R^2	0.974	0.922	0.914	0.901	0.961	0.954
	Δq, %	84.54	57.36	46.89	189.2	68.92	77.72

is between 0 and 1, which indicates that the adsorption of is favorable for both colorants [Riza et al., 2020; Hou et al., 2021; Othaman et al., 2018]. Furthermore, with the DR model, the energy required to adsorb a molecule from the sinus of the solution increases its value with increasing temperature, following the behavior shown in Figure 1, for both dyes.
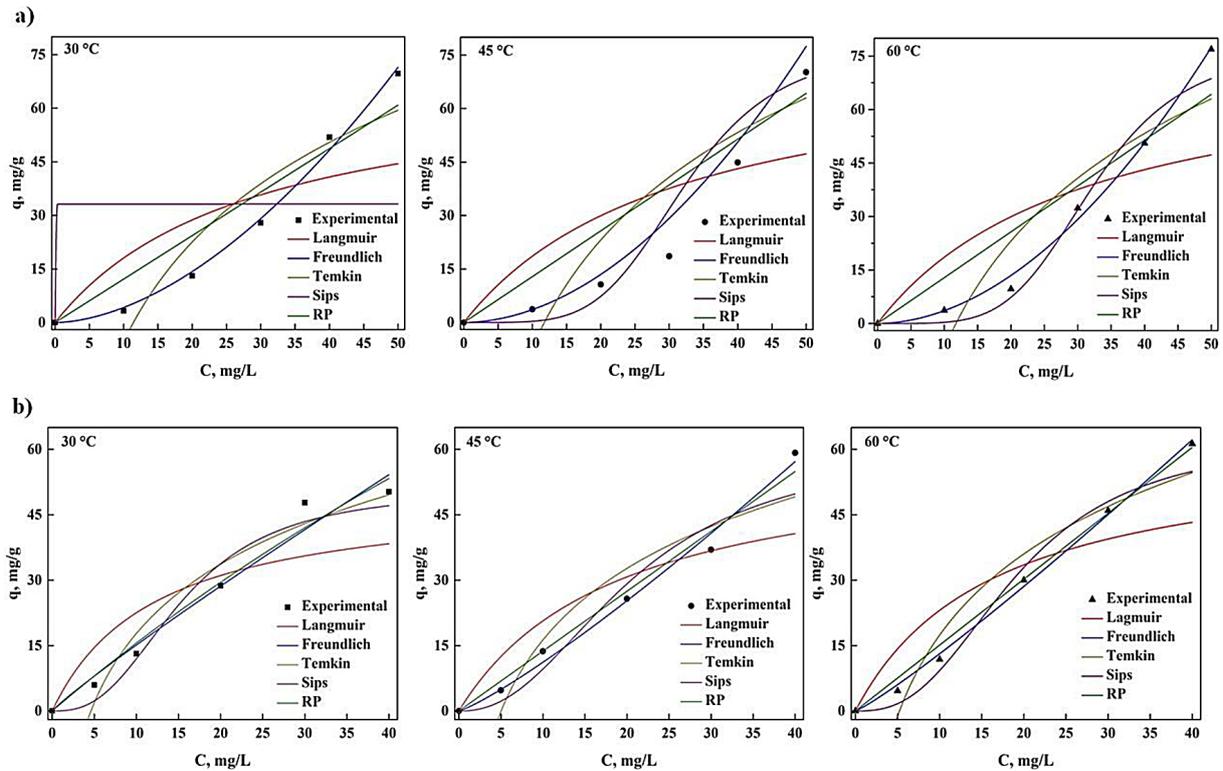

Figure 2. Equilibrium data for dye adsorption using WLN: a) MB and b) MO

Table 4. Parameters of the isotherm models in the adsorption of MB and MO with WLN

Models	Parameter	MB			MO		
		T			T		
		30°C	45°C	60°C	30°C	45°C	60°C
Langmuir	K_L	0.035	0.056	0.073	0.053	0.057	0.061
	q_m	70.034	62.69	58.83	60.03	57.895	61.03
	R_L	0.84-0.32	0.79-0.32	0.73-0.26	0.79-0.32	0.78-0.30	0.77-0.29
	R^2	0.673	0.529	0.539	0.806	0.801	0.801
	Δq, %	1.735	39.89	92.09	61.73	7.125	1.291
Freundlich*	K_F	0.074	0.049	0.044	0.989	0.799	0.741
	n	0.571	0.538	0.524	0.941	0.855	0.835
	R^2	0.995	0.993	0.995	0.998	0.954	0.990
	Δq, %	0.321	1.968	2.907	2.271	4.653	0.857
SIPS	K_S	0.014	0.028	0.031	0.052	0.065	0.048
	q_m	67.55	70.75	77.74	62.75	50.75	60.75
	n_S	0.001	6.147	4.673	2.669	2.087	2.295
	R^2	0.241	0.961	0.974	0.977	0.970	0.937
	Δq, %	11.58	3.123	4.361	78.83	21.08	2.943
DR	q_m	106.1	141.3	177.8	68.29	66.05	67.22
	k_{DR}	178.77	287.5	321.7	61.11	55.87	47.33
	E, J/mol	52.88	41.7	31.42	94.60	91.86	90.46
	R^2	0.979	0.968	0.931	0.861	0.898	0.946
	Δq, %	194.9	379.7	514.8	34.05	40.31	113.8

Figure 2 shows the adsorption of MB and MO using WLN at different temperatures, in which it is shown that the removal of both dyes increases along with temperature due to the treatment carried out in WLN, this being the opposite behavior to what is seen in the samples treated with water, favoring the adsorption of the dyes at high temperature. The adsorption data in equilibrium adjusting them to the isotherm models (Figure 2) described in Table 1, using the criteria of R^2 and Δq%, the best fit of the isotherm models shown in the following table can be chosen.

The results shown in Table 4 showed that the best model that fits the experimental data is Freundlich for the two dyes at any temperature: this model indicates that the adsorption of the dye molecules is carried out by means of a chemical process. This allows having heterogeneity on the surface of the bioadsorbent, in addition to having favorable adsorption, since 1/n is between 1 and 10. On the other hand, the DR model found that the energy required to adsorb a molecule from the sine of the solution decreases its value with increasing temperature, following the behavior shown in Figure 2, for both colorants.

There is a great plurality of opinions in the literature on the best isotherm model that is coupled to the behavior of adsorption in the adsorption of these dyes, as well as various materials used. In Table 5 the adsorption capacity of different adsorbents was compared and it was observed that the adsorption capacity of our adsorbent is within the reported values. In the specific case of *E. crassipes* it is shown that there is practically the same maximum value of the adsorption capacity reported together with the low temperature (around 25 °C). What can be mentioned is that there is an adsorbent capable of having an adsorption capacity similar to the other adsorbents and a behavior similar to that of several studies previously carried out (Freundlich model). These last results agree with what was observed in this work with the water and NaOH treatments with the experimental data modifying the structure of WL. The analysis of the obtained results with the literature means that the adsorption capacity of the employed adsorbent is within the reported values, which is why it can be considered that the study of the modified surface is necessary to be able to compare with other adsorbents.

Thermodynamic analysis of the of MB and MO adsorption process

The nature of the process of MB and MO elimination was analyzed by means of the thermodynamic parameters that are shown in Table 6. It can be observed for the case of the MO and MB adsorption with WLW that the spontaneous process ($\Delta G < 0$), being that the Gibbs free energy decreases with increasing temperature and there is an exothermic process ($\Delta H < 0$), confirms what was observed in the adsorption isotherms, i.e. that the adsorption capacity decreases with increasing temperature, leaving MO adsorption where higher energy is released compared to MB removal. In addition, there is a change in randomness in the fluid-solid interface ($\Delta S > 0$) in the elimination process, being more noticeable in the adsorption of MO in WLW. The process of removal MB and MO using WLN was analyzed through the thermodynamics of the process for which the parameters shown in Table 6 were determined, where the Gibbs free energy decreases with increasing temperature and indicates that the process is spontaneous ($\Delta G < 0$), but the removal has an endothermic nature ($\Delta H > 0$), which confirms what was observed in the adsorption isotherms that the adsorption capacity increases along with temperature, being MO adsorption where higher energy is adsorbed compared to the MB removal. There is a change in randomness in the fluid-solid interface ($\Delta S > 0$) in the elimination process, being more noticeable in the MO adsorption.

The nature of the MB and MO removal process has been widely reported in the literature with different adsorbents where it is mentioned that the process is spontaneous for all these works [Riza et al., 2020; Jedynak et al., 2021; Zaghoul et al., 2021], but in the case of ΔH, it is only reported for nanoparticles, mesopore carbons and hydrogel [Anastopoulos et al., 2017; Jedynak et al., 2021; Riza et al., 2020] they have an endothermic nature for MB and MO, respectively, which in the obtained results are consistent with WLN. In other studies, it was determined that there is an exothermic process where modified hydroxyapatites are used as adsorbents [Guan et al., 2018], biochar from *E. crassipes* [Nurhadi et al., 2019], chitosan/cellulose [Xu et al., 2021], biochar with pineapple leaves [Soltani et al., 2021)] and MgAl [Zaghoul et al., 2021] this behavior is what was determined for the WLW adsorbent. In the case of the randomness of the solid/liquid interface in the

Table 5. Comparison of the adsorption capacity in equilibrium of MB and MO using various adsorbents

Adsorbent	Dye	q, mg/g	Model	Reference
ZnO-NiO with different Zn/Mg ratios	MB	228	Langmuir	(Alguacil et al., 2021)
Halloysite clays		10		(Filie et al., 2021)
Chitosan/cellulose		122.7		(Xu et al., 2021)
Rice husk		17.78		(Azam et al., 2020)
Activated carbon mesopores		330		(Jedynak et al., 2021)
MCM-41 mesopores		55		(Ríos et al., 2019)
Biocarbon obtained from sapote leaves		60		(Herrera-González, 2019)
Wheat husk treated with acrylamide and citric acid		120.84		(Liu et al., 2019)
Hydroxyapatite modified with chitosan-montmorillenite		137.5		(Joudi et al., 2020)
E. crassipes treated with HCl		260	Freundlich	(Priya et al., 2017)
Fe_3O_4/MCM-41		1374		(Anaspolos, 2017) (Tara, 2020)
		14.33		(Othman, 2018)
Biochar		113-841.6		(Azam et al., 2020; Geed et al., 019; Srivatsav et al., 2020)
E. crassipes treated with water		7.95		(Wanyonyi et al., 2013)
E. crassipes treated with water		103.42		(Prasad et al., 2021)
Biochar (*E. crassipes*) treated with H_3SO_4		19.48		(Nurhdi et al., 2019)
Roots, leaves and stems of *E. cassipes*		8.6–128.9		(Priya et al., 2014)
E. crassipes was modified with $NaIO_4$-NC		90.91		(Tsade-Kara, (2021)
WLW.	-	95.7		This work
WLN	-	78.4		
ZnO-NiO with different Zn/Mg ratios	MO	4.4	Langmuir	(Alguacil et al., 2021)
Halloysite clays		4		(Filie et al., 2021)
Lotus roots		44.2		(Huo et al., 2021)
Rice husk		15.21		(Azam et al., 2020)
Activated carbon mesopores		222		(Jedynak et al., 2021)
Wheat husk treated with acrylamide and citric acid		3053.48		(Liu et al., 2019)
Hydroxyapatite modified with chitosan-montmorillenite		168.52		(Joudi et al., 2020)
Hellosite clay		14.96	Sips	(Lacin et al., 2020)
Nanoparticles of Ag, Fe_3O_4, Ni, among others		23.21-849.3	Freundlich	(Tara et al., 2020)
Swieteia mahagoni treated with NaOH		16.87		(Ghosh et al., 2020)
WLW.		76.9		This work
WLN		61.3		

Table 6. Thermodynamic parameters of MB and MO adsorption process with WLW and WLN

T, °C	−ΔG, kJ/mol	−ΔH, kJ/mol	ΔS, kJ/mol K	−ΔG, kJ/mol	ΔH, kJ/mol	ΔS, kJ/mol K
MB (WLW)				MB (WLN)		
25	35.89			33.82	-	-
35	36.76	17.46	0.0607	36.38	4.11	0.129
45	37.71			38.97	-	-
MO (WLW)				MO (WLN)		
25	35.57			34.71	-	-
35	36.66	14.53	0.0694	35.64	18.25	0.172
45	37.65			38.55	-	-

adsorption process, for MB and MO, it was necessary that for MgAl and chitosan/cellulose [Zaghoul et al., 2021; Xu et al., 2021] as adsorbents present a decrease in randomness ($\Delta S < 0$): on the other hand, there is greater randomness using oxide nanoparticles [Anastopoulos et al., 2017], hydrogels [Riza et al., 2020], modified hydroxyapatite [Guan et al., 2018], and biochar from *E. crassipes* [Nurhadi et al., 2019]. These results confirm what is determined in this study for the MB and MO adsorption for both treatments.

Effect of the bioadsorbent concentration on the removal of MB and MO

The analysis that was carried out to the kinetic adsorption process of the dyes firstly consisted in the relationship that existed between the amount of bioadsorbent (C_{ads}) pretreated with the removal of each of the dyes shown in Figure 3, where it can be seen that the adsorption capacity of MB and MO decreases with increasing concentration of the bioadsorbent. This is reflected in the percentage of MB removal captured on the surface of WLW (Figure 3a) where there is between 80.3 and 98% removal at 30 °C and from 46.3 to 50% at 60 °C, when it has a concentration of 1 to 5 g/L, respectively. Regarding the temperature, at 30 and 45 °C, they it reaches 98 and 92% of maximum removal, respectively; however, at 60 °C this percentage decreased by almost 50%, compared to the other two temperatures. In the case of the adsorption of MB with WLN (Figure 3c), it can be observed that the treatment with NaOH helped in the maximum adsorption capacity of the dye and, consequently, in the removal of MB, since the variation of the removal percentage at different bioadsorbent concentrations became narrower, that is, there is an elimination percentage that ranges from 91 to 97% between 1 and 5 g/L. Furthermore, it was also found that the effect of temperature on the maximum adsorption capacity for both treatments is the same as that shown in the study carried out in equilibrium. For the MO adsorption capacity, it is shown that it decreases with increasing concentration of the bioadsorbent. This directly affects the percentage using WLW (Figure 3b) where there is between 56.7 and 82.8% of removal at 30 °C and from 48.1 to 56.7% at 60 °C, when there is a concentration of 1 to 5 g/L, respectively. Regarding the temperature, at 30 and 45 °C, they reach 67 and 65% of maximum removal; however, at 60 °C

the percentage decreased to 56.7%. For the adsorption of MO with WLN (Figure 3d), it can be observed that the treatment with NaOH, improved the maximum capacity of MO adsorption and removal, since the variation of the removal percentage at the different concentrations of bioadsorbents was from 60 to 87.7% between 1 and 5 g/L at 60 °C. As in MB adsorption, the effect of temperature on the maximum adsorption capacity for both treatments in the same as that shown in the study carried out in equilibrium.

The effect that occurs with the concentration of the adsorbent of the dyes on the removal percentage and adsorption capacity among them is mentioned in several works, e.g. reported by Bożęcka [2021] where they used walnut, sunflower and rice shells, obtaining a removal percentage of various dyes up to 99%. Kakhki [2020] observed that by modifying the amount of mass of its adsorbent in the solution, the removal percentage of MO increases until obtaining 90%, although this causes a significant decrease in the adsorption capacity. This behavior was observed using mesoporous activated carbon [Azam et al., 2020] for the adsorption of MB and MO, it was found that the adsorption capacity decreases with the increase of Cads, causing an increase in the removal of dyes (98.5% for MO and 82% for MB). Moreover, the use of biochar from natural sources such as black sapote leaves [Herrera-González et al., 2019], *E. crassipes* [Nurhadi et al., 2019], Spirulina algae residues [Zhu et al., 2021], chestnut hull [Zhang et al., 2018] lychee seeds, banana peel [Srivatsav et al., 2020] obtaining in these works a removal percentage of 66.7 up to 99.9% for both dyes.

In another report [Othman et al., 2018] where Fe_3O_4 nanoparticles are also used for MB adsorption, it was shown that by increasing the adsorbent concentration, a removal of 99.6% is achieved and when hydroxyapatite with chitosan/montmorillonite is used [Jaudi et al., 2020] there is a 99.9% removal for MO and 80% for MB. Likewise, for the removal of MB using the *E. crassipes* treated with water [Prasad et al., 2021; Wanyonyi et al., 2013] there is a percentage of elimination between 79 and 99%, mentioning that this removal is favored with the amount of mass of the adsorbent in solution. There are studies that report the adsorbers that have been pretreated to improve the adsorption capacity, as well as the removal of MB and MO, including *Swietenia mahagoni* [40] that was treated with NaOH, noting that the percentage of MO removal increases from 34 to 98%

with the increase in C_{ads} but the adsorption capacity decreases from 6.87 to 0.65 mg/g; the same case happens with pretreated used coffee powder [47] where 100% removal was achieved for MB and MO and also in the case of the biochar obtained from the grapefruit peel treated with H_3PO_4 [2] where the adsorption capacity decreases from 89.35 to 9.99 mg/g increasing C_{ads} from 1 to 10 g/L. For the *E. crassipes* treated with H_2O_2 and later covering it with ZnO [48] for various dyes, this behavior was demonstrated where removal decreases due to decreasing the concentration of the adsorbent causing the adsorption capacity to increase significantly up to a 94.6%.

In general, this behavior may be due to the fact that the increase in the concentration of the bioadsorbent creates a higher concentration of active sites available for the removal of the dyes [Gosh et al., 2020; El-Zawahry et al. 2016], inferring the amount of the adsorbent is adequate, avoiding the sites are not blocked on the surface, this may be directly influenced by the increase in randomness in the fluid-solid interface present in the surfaces treated with water and NaOH, considering that the adsorption capacity of the dyes is influenced inversely proportional to the amount of mass of the adsorbent is what causes the loss of adsorption.

Kinetic study of MO and MB removal

The analysis of MB adsorption kinetics using WLW was carried out to determine the process that controlled the removal of the dye by fitting the experimental data to the different kinetic equations (Table 2). The parameters of each of these models are presented in Table 7, where both the deterministic coefficient (R^2) and normalized standard deviation ($\Delta q\%$) were taken to choose the best fit, i.e. the PSO, which reveals that the adsorption of the MB molecules is carried out on the surface of the bioadsorbent through the use of two active sites, which must have been widely available to remove MB from the solution. Taking this analysis into account, it can be determined that there are no internal and external mass transfer limitations, since these models are the ones that showed a less favorable fit compared to the others. The maximum adsorption capacity of MB is presented at 30 °C (200.8 mg/g), This value as the temperature increases, at 45 and 60 °C, there is an adsorption capacity of 155.7 and 115.5 mg/g, respectively. This result confirms the nature of MB adsorption that was found in the equilibrium study, since there is an exothermic process.
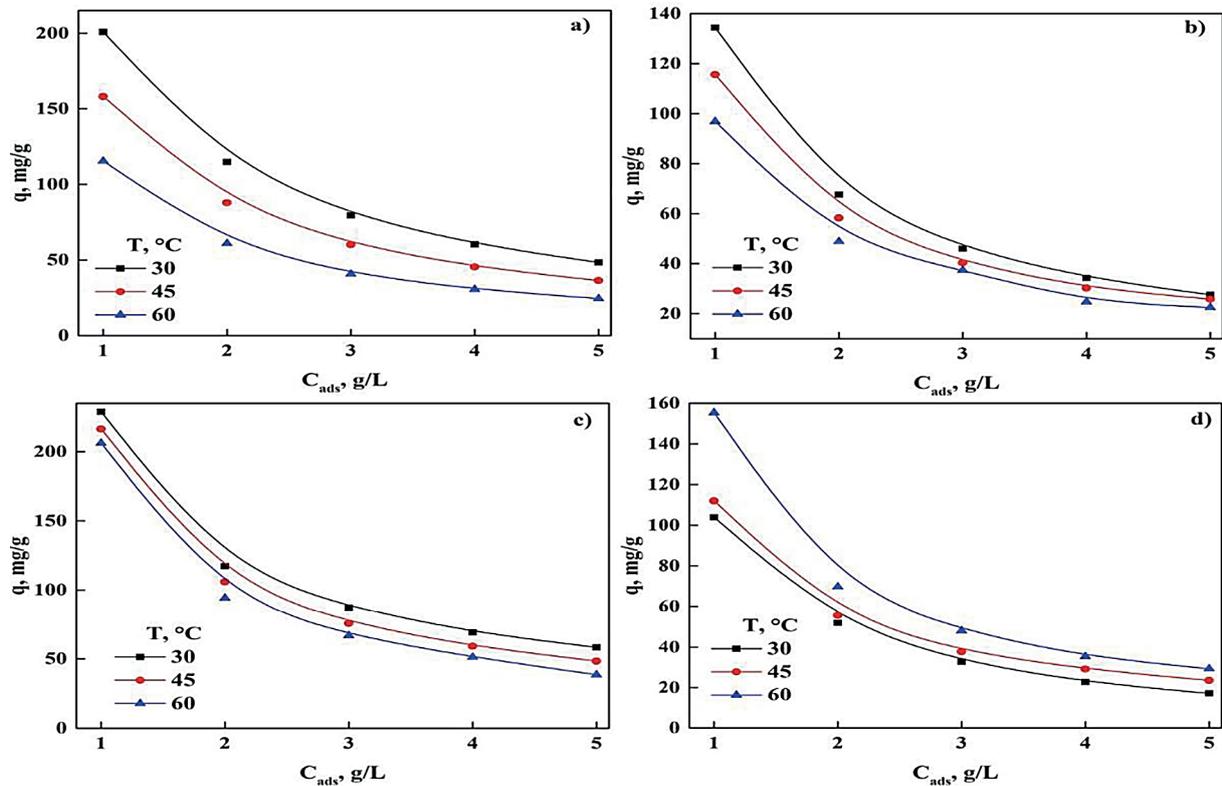

Figure 3. Effect of the amount of bioadsorbent on the adsorption of MB and MO:
a) MB-WLW, b) MO-WLW, c) MB-WLN and d) MO-WLN

Table 7. Kinetic parameters for MB adsorption with WLW

Model		1 g/L			2 g/L			3 g/L		
		30°C	45°C	60°C	30°C	45°C	60°C	30°C	45°C	60°C
PFO	q_{max}, mg/g	204.89	157.74	115.45	121.18	109.08	64.682	84.004	72.024	42.952
	k_1, h⁻¹	0.8105	0.8901	0.8561	0.7802	0.7471	0.7403	0.8205	0.7941	0.8704
	R^2	0.9032	0.9533	0.9601	0.9090	0.9089	0.9584	0.9231	0.9145	0.9333
	Δq, %	0.0118	1.2559	0.6741	2.6751	2.6775	1.6508	2.3462	2.4772	3.4612
PSO	q_{max}, mg/g	200.49	155.34	111.19	61.221	104.89	64.355	79.563	69.563	45.856
	k_2, h⁻¹	0.3196	0.0429	0.0164	0.3515	0.1421	0.0491	0.6752	0.4102	0.1018
	R^2	0.9998	0.9993	0.9915	0.9999	0.9997	0.9966	0.9999	0.9999	0.9985
	Δq, %	0.0037	0.2311	0.0931	0.1383	0.2184	0.1893	0.0601	0.0196	1.3227
Elovich	α, mg/g	100.01	514.23	568.03	90.034	65.295	78.945	152.90	60.976	79.045
	β, mg/g*h	0.1147	0.0204	0.0221	0.1862	0.0437	0.0451	0.1091	0.0699	0.0699
	R^2	0.9896	0.8759	0.9342	0.9861	0.9124	0.9603	0.8781	0.9521	0.9255
	Δq, %	2.0315	5.2977	3.0957	2.2032	4.9289	3.8109	4.6681	4.6502	4.6502

Table 8. Kinetic parameters for MO adsorption with WLW

Model		1 g/L			2 g/L			3 g/L		
		30°C	45°C	60°C	30°C	45°C	60°C	30°C	45°C	60°C
PFO	q_{max}, mg/g	152.36	131.04	90.484	66.711	65.831	46.296	57.432	44.629	36.568
	k_1, h⁻¹	0.6474	0.8701	0.8403	0.8421	0.7401	0.5624	0.7561	0.8911	0.4501
	R^2	0.8664	0.9613	0.9613	0.9486	0.9215	0.9482	0.9605	0.9595	0.9653
	Δq, %	9.5356	1.3691	3.3822	3.3822	1.9764	2.4187	1.3205	1.2328	1.0020
PSO	q_{max}, mg/g	193.51	127.41	97.871	66.321	63.272	48.961	45.981	43.461	37.401
	k_2, h⁻¹	0.0031	0.0627	0.0158	0.0711	0.1289	0.0232	0.1053	01959	00263
	R^2	0.9905	0.9993	0.9962	0.9811	0.9993	0.9911	0.9971	0.9988	0.9856
	Δq, %	0.0347	0.0911	0.0077	0.8764	0.1611	0.0151	0.0057	0.0286	0.0072
Elovich	α, mg/g	461.31	87.702	63.751	72.345	55.456	116.45	48.912	58.111	53.755
	β, mg/g*h	0.0301	0.0417	0.0611	0.0915	0.0854	0.0962	0.1293	0.1411	0.1063
	R^2	0.9121	0.9457	0.9831	0.9446	0.9387	0.9823	0.9779	0.9613	0.9873
	Δq, %	0.5807	4.1728	0.8537	1.4419	3.9297	0.9021	3.0056	3.4983	0.4059

In the case of MO adsorption in WLW, the kinetic parameters of the different models that were used to adjust the data obtained from the experimentation shown in Table 8. Using the deterministic coefficient (R^2) and the normalized standard deviation (Δq%) to choose the best fit, it was found that the PSO model is the one that gives an excellent fit compared to the other models, which reveals that the MO removal process is carried out by using the active sites on the surface in proportion of two sites for each dye molecule, It can also be inferred that the adsorbent has a wide availability of these sites in its surface perimeter to carry out the removal of MO from the solution.

Furthermore, there are no external and internal mass transfer problems because these models do not adequately fit the experimental data, leaving the process to depend on other factors. The maximum MO adsorption capacity was found at 30 °C (134.37 mg/g) which decreases as the temperature increases, since at 45 and 60 °C there is an adsorption capacity of 126.7 and 96.92 mg/g, respectively. This confirms what was discovered in the equilibrium analysis of MO adsorption using WLW which is an exothermic process in nature.

The kinetic process of adsorption of MB using WLN was carried out to deterine if modifying the surface of WL with NaOH follows the same process that controls the removal of the dye by means of which the experimental data were adjusted with the different kinetic equations (Table 2). The parameters of each of these models are presented in Table 9, where the deterministic coefficient (R^2) and normalized standard deviation (Δq%) were used as criteria to choose the best fit, which corresponds to the PSO for this process. This reveals that the adsorption of the MB molecules is carried out on the surface of the bioadsorbent through the use of two active sites. It must have had a wide availability of these sites

to carry out the removal of MB from the solution. Furthermore, with this analysis of the different models, it was found that there are no external and internal mass transfer problems, since the adjustment is the least favorable compared to the others. The maximum adsorption capacity of MB occurs at 60 °C (228.5 mg/g) which decreases slightly as the temperature decreases. At 45 and 30 °C there is an adsorption capacity of 227.5 and 226.1 mg/g, respectively. This result shows that the modification suffered in the surface treated with NaOH increases the adsorption capacity by 14%, in addition to changing the nature of MB adsorption, since in the treatment with water it is an exothermic process and with NaOH it is an endothermic process.

In the removal of MO in WLN, the kinetic parameters of the different models were determined and used to adjust the data obtained from the experimentation, shown in Table 10. Using the deterministic coefficient (R^2) and the normalized standard deviation ($\Delta q\%$) to choose the best fit, it was found that the PSO model is the one that gives an excellent fit compared to the other models. This reveals that the MO removal process is carried out by using the active sites in the surface in a proportion of two sites for each molecule of dye. It can also be inferred that the adsorbent has a wide availability of these sites on its surface perimeter to carry out the removal of MO from the solution. In addition, there are no external and internal mass transfer problems because these models do not adequately fit the experimental data, leaving the process to depend on other factors. The maximum MO adsorption capacity was found at 60 °C (155.4 mg/g) which decreases as the temperature increases, since at 45 and 30 °C there is an adsorption capacity of 112 and 104 mg/g, respectively. The result shows that the modification of the surface treated with

Table 9. Kinetic parameters for MB adsorption with WLN

Model		1 g/L			2 g/L			3 g/L		
		30°C	45°C	60°C	30°C	45°C	60°C	30°C	45°C	60°C
PFO	q_{max}, mg/g	226.91	239.42	246.37	115.98	121.18	124.42	81.346	82.626	83.564
	k_1, h^{-1}	0.8911	0.7812	0.6843	0.8911	0.7885	0.7632	0.8976	0.8765	0.8199
	R^2	0.9564	0.9191	0.8839	0.9311	0.9093	0.9216	0.9478	0.9345	0.9214
	Δq, %	0.0888	2.5998	3.4053	0.0329	2.6999	2.7434	1.5366	2.1912	2.5211
PSO	q_{max}, mg/g	226.48	230.62	236.62	114.42	115.89	117.25	78.873	78.825	79.356
	k_2, h^{-1}	0.0466	0.0808	0.1112	0.3426	0.2028	0.1802	0.1543	0.7505	0.4304
	R^2	0.9988	0.9999	0.9999	0.9979	0.9998	0.9994	0.9997	0.9999	0.9999
	Δq, %	0.0058	0.3296	0.0091	0.0526	0.0003	0.0113	0.1304	0.0332	0.1423
Elovich	α, mg/g	59.611	69.513	68.934	59.056	67.545	61.234	56.978	45.643	53.126
	β, mg/g*h	0.0179	0.0186	0.0182	0.0419	0.0438	0.0415	0.0685	0.0631	0.0652
	R^2	0.8831	0.8683	0.8683	0.9046	0.9029	0.9104	0.9307	0.8991	0.9097
	Δq, %	5.6383	5.8231	6.0052	5.1482	5.1656	5.1656	4.3121	5.2773	5.0647

Table 10. Kinetic parameters for MO adsorption with WLN

Model		1 g/L			2 g/L			3 g/L		
		30°C	45°C	60°C	30°C	45°C	60°C	30°C	45°C	60°C
PFO	q_{max}, mg/g	119.84	120.87	172.15	66.615	55.703	50.756	40.931	34.349	31.214
	k_1, h^{-1}	0.4508	0.4798	0.4122	0.4107	0.3121	0.4031	0.5208	0.4536	0.5011
	R^2	0.9530	0.9269	0.9437	0.8728	0.8311	0.9434	0.8565	0.8993	0.9234
	Δq, %	3.8931	3.2245	2.7606	5.4353	8.7811	3.2345	4.2653	3.7026	3.9242
PSO	q_{max}, mg/g	158.36	121.79	104.39	67.935	55.723	50.984	41.872	34.788	30.923
	k_2, h^{-1}	0.0132	0.0219	0.0149	0.0346	0.0424	0.0305	0.1328	0.0703	0.0697
	R^2	0.9933	0.9901	0.9826	0.9992	0.9982	0.9922	0.9999	0.9926	0.9932
	Δq, %	0.0022	0.0175	0.0022	2.9431	0.0227	0.0175	1.0165	0.0243	0.1283
Elovich	α, mg/g	57.745	42.978	150.06	75.123	126.87	175.66	45.983	279.98	123.89
	β, mg/g*h	0.0301	0.0429	0.0351	0.1316	0.0741	0.0942	0.1804	0.1512	0.1268
	R^2	0.9764	0.9866	0.9741	0.9943	0.9741	0.9927	0.9698	0.9928	0.9754
	Δq, %	2.6246	2.4671	2.3682	1.7415	2.3682	0.9243	3.2515	1.7515	2.6461

Table 11. Comparison of the adsorption capacity of MB and MO using various adsorbents

Adsorbent	Dye	q, mg/g	Model	Reference
Nanoparticles of various oxides	MB	14.33–875.5	PSO	(Anastopoulos et al., 2017; Othman et al., 2018)
Coconut shell, lychee, Chestnut and *Spirulina algae* residues pretreated with different methods		5–1489.88		(Geed et al., 2019; Srivatsav et al., 2020; Zhu et al., 2021; Zhang et al., 2018)
Chitosan/cellulose		213		(Xu et al., 2021)
Helloysite clay Hydroxyapatite-chitosan/montmorillon-ite mesoporous carbons		10–222		(Filice et al., 2021; Joudi et al., 2020; Jedynak et al., 2021)
E. cassipes washed with water		7.95–161.64		(Mishra et al., 2017; Wanyonyi et al., 2013; Prasad et al., 2021)
Biochar from *E. cassipes*		19.48		(Nurhadi et al., 2019)
WLW	-	200.8	-	This work
WLN	-	228.5	-	This work
Salvinia molesta	MO	12.5	PFO	(Al-Baldawi et al., 2020)
Grapefruit peel MgAl Hydrogels Cu-coated nanoalum Lotus root biochar		7–330	PSO	[Zhang et al., 2019; Zaghloul et al., 2021; Riza et al., 2020; Kakhki et al., 2020; Lacin et al., 2020; Hou et al. 2021]
Helloysite clay Hydroxyapatite-chitosan/montmorillon-ite mesoporous carbons		8–330		(Filice et al. 2021; Joudi et al. 2020; Jedynak et al. 2021)
WLW	-	134.37	-	This work
WLN	-	155.4	-	This work

NaOH increases the adsorption capacity by 16%, in addition to changing the nature of the MO adsorption, that is, with the treatment with water it is an exothermic process and with the treatment with NaOH it is endothermic in nature.

Comparing the obtained results with those reported in the literature (Table 11), it was observed that the adsorption capacity of WLW and WLN is similar with most of these materials, but there is greater adsorption of the employed biomaterial compared to the works where they have used *E. crassipes* with respect to MB adsorption. In the removal of MO using WLW and WLN with the materials, a comparable adsorption capacity was obtained with them using a simple and cheap pretreatment; however, there is no study that relates the Water Lily to the removal of MO.

Characterization of WL with the different pretreatments

Figure 4 shows the micrographs of WL with the two treatments used to study the adsorption of MB and MO, where it could be observed that there are irregular surfaces, with porosity, with cavities for the WLW adsorbent (Figure 4a), in the case of WLN, it was observed that

it has rough surfaces together with pores and fractures in the structure due to treatment with NaOH (Figure 4b), the presence of pores on both surfaces indicates that there is a good probability that the dyes could be adsorbed on the surface [Giri et al., 2012; El-Zawahry et al., 2016; Nurhadi et al. 2019].

In the MB adsorption in WLW (Figure 5a), it was observed that there is a smooth surface, which confirms that MB is being trapped. This may be due to surface precipitation. In the case of MO adsorption, it is observed in Figure 5b. It can be noticed that there are clusters of dye in the cavities of the surfaces of *E. crassipes* and no a significant change in the surface can be noticed; however this does not imply that there is a good adsorption since the adsorption results for both dyes are very encouraging to be able to use *E. crassipes* as a natural adsorbent in addition to considering it in phytoremediation [Prasad et al., 2021; Tabinda et al., 2019; Rashid et al., 2019]. The micrographs of the MB and MO adsorption are shown in Figure 6, which – due to the treatment with NaOH – have a fibrous surface with fractures and perceptibly more porous compared to WLW. In the figure, it was possible to observe

that in the cavities the clusters of dyes adsorbed on the surface are deposited.

The diffractograms of *E. crassipes* with and without treatment are shown in Figure 7, where the peaks (flat) can be observed in WLW 14.7 (1 1 0), 21.9 (2 0 0), 24.3 (0 0 4), 28.3, 40.5, 50, 58.5, 66.3 and 73.68°, the first 3 peaks refer to amorphous cellulose, the next peak is the characteristic pattern of WL and the other peaks are assigned to the presence of calcite in the adsorbent [Bronzato et al., 2017; Nurhadi et al., 2019; Tsade-Kara et al., 2021]. Comparing this pattern with the other samples treated with water, it can be observed that there are no significant changes in the crystalline structure when

water was used, instead in the WLN sample where the peaks between 40 and 80° disappear, there is an additional decrease in intensity of the peaks at 40.5, 28.3 and 24.3, with a change in the width of the peak, indicating that there is a change in the crystallinity of the sample or the elimination of lignin in WL [Bronzato et al., 2017; Nurhadi et al., 2019].

After the adsorption of MB and MO in both adsorbents treated with water and NaOH (Figure 8), it was noted that the removal of the dyes significantly increased the crystallinity of WLW as practically all the peaks disappeared except at 14.7° and it was also observed that the width of the peak centered at 21.9° [Bronzato et al., 2017;
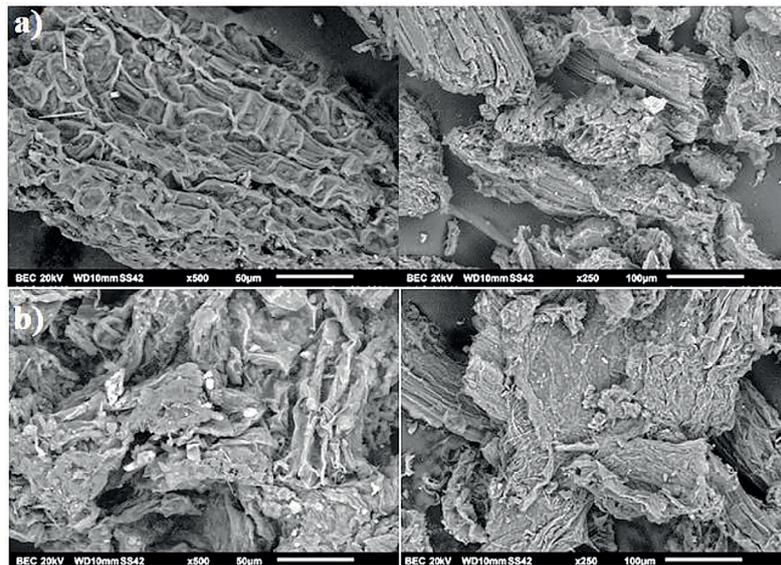
Figure 4. SEM micrographs of WL: a) WLW and b) WLN
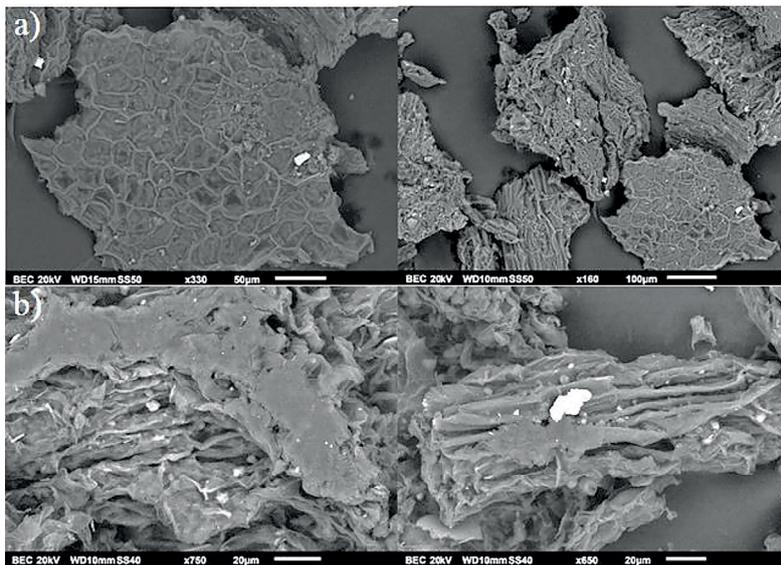
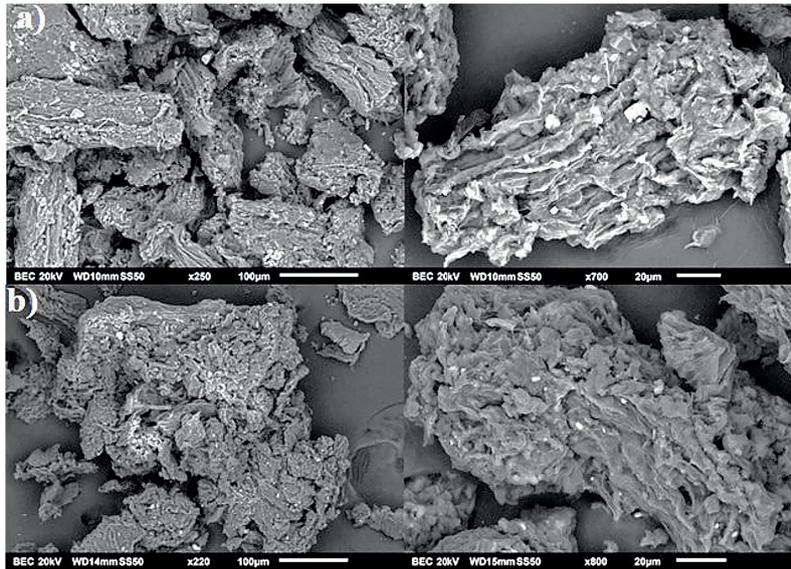**Figure 5.** SEM micrographs of WLW after dye adsorption: a) MB and b) MO

Figure 6. SEM micrographs of WLN after adsorption of the dyes: a) MB and b) MO
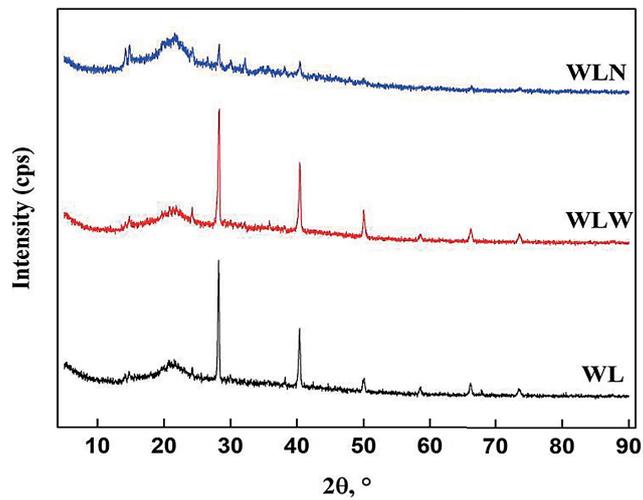

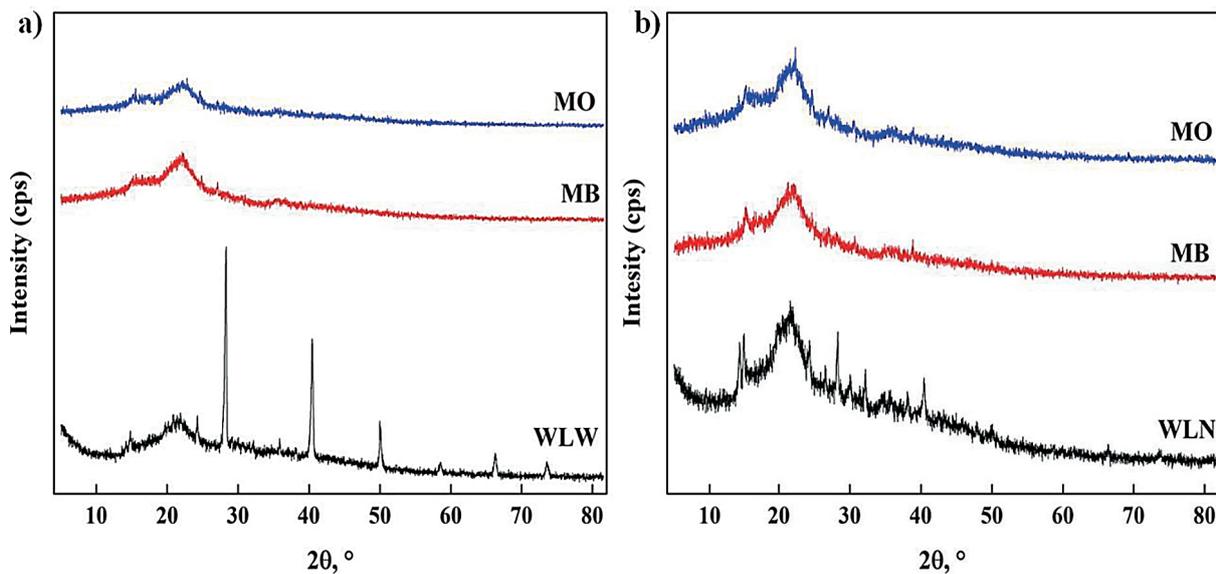**Figure 7.** WL XRD patterns with different pretreatments

Figure 8. XRD patterns after adsorption of dyes: a) WLW and b) WLN

Tsade-Kara et al., 2021], in the case of WLN due to the treatment, a change in crystallinity was observed and comparing the results obtained both in kinetics and adsorption isotherm, it can be inferred that the crystallinity of the sample favors the adsorption of MO and affects the removal of MB.

In Figure 10, the ATR-FTIR of *E. crassipes* with their different treatments is shown, where the spectrum of WL without treatment shows different bands that are assigned to different functional groups. At 3300 cm^{-1} corresponds to the vibrational mode of stretching of the hydroxyl group -OH, as
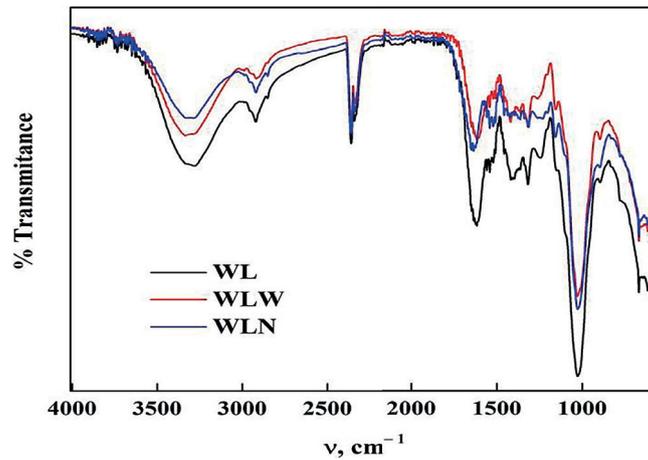
Figure 9. ATR-FTIR spectra of WL with the different pretreatments
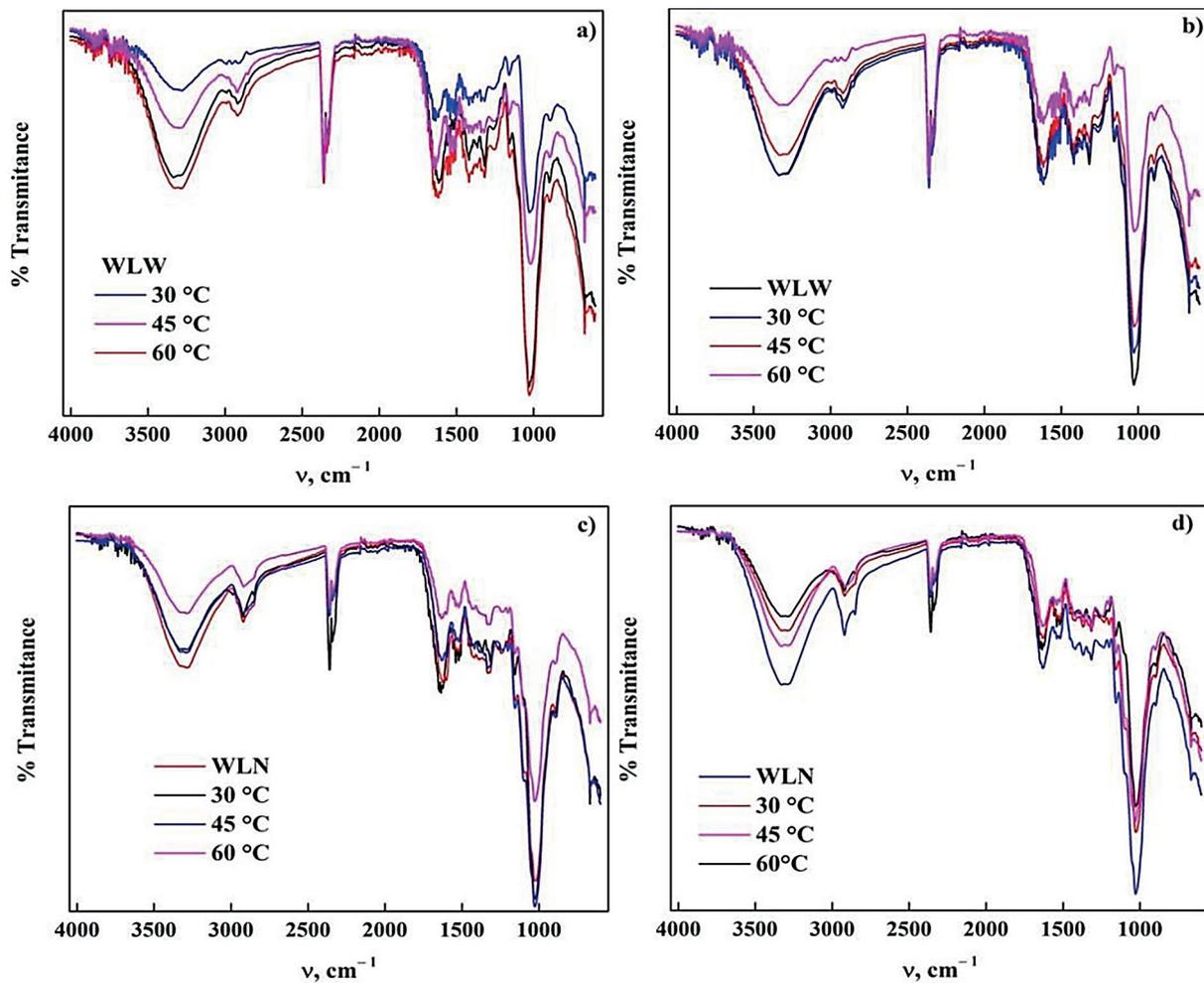
Figure 10. ATR-FTIR spectra of WL after adsorption to the dyes: a) WLW-MB, b) WLW-MO, c) WLN-MB and d) WLN-MO

well as the bonds of cellulose and lignin, the band at 2924 cm^{-1} is assigned the vibration of asymmetric stretching and symmetry of the C-H group of the methyl groups and methylene [Bronzato et al., 2017; Prasad et al., 2021]. The peak at 1615 and 1528 cm^{-1} correspond to the presence of stretching vibrations of the carboxylic group C=O of different groups and to lignin, respectively [Bronzato et al., 2017; Prasad et al., 2021; Tsade-Kara et al., 2021], while at 1313 cm^{-1} it is due to the vibration of the symmetric stretching of COO-, the peak at 1246 cm^{-1} can be attributed to the aromatic C-O group and at 1018 cm^{-1} is due to the stretching vibration C-OH of alcoholic groups, carboxylic acid and lignin [Bronzato et al., 2017; Prasad et al., 2021]. At 671 cm^{-1} it is assigned to the ß-glucosidic bonds between glucose units of cellulose.

In Figure 9, is observed that in the bands assigned to lignin (3300, 1610, 1528, 1246 and 1018 cm^{-1}) their intensity decrease significantly for both treatments, but in WLN this decrease is more pronounced, which indicates that NaOH removes the lignin allowing the sample to have higher crystallinity compared to WLW. In Figure 10, the change in intensity and location of the bands was observed when participating in the adsorption of MB and MO at different temperatures.

MB is a cationic dye, therefore acidic functional groups such as -OH, CH, C = O, COO-, CO and COH tend to participate in adsorption due to the fact that the dye has a positive charge, so it is attracted by these functional groups, as observed in Figure 10a. It is also observed that at 30°C, the participation of these groups is notorious, since its intensity decreases, in the case of MO adsorption, although there is a similar behavior, the participation is lower because the intensity of these groups does not decrease when buying with the removal of MB in WLW [Prasad et al., 2021; Tsade-Kara et al., 2021]. For the removal of both dyes using WLN, there is a participation of these same groups favoring the adsorption of MO, contrary to the elimination of MB with WLW, this indicates that there is a strong interaction between the electrostatic forces of the materials with the dyes, since the treatment modified the surface of these [Bronzato et al., 2017; Prasad et al., 2021; Tsade-Kara et al. 2021]. To corroborate this, the isoelectric point (pHzpc) of WLW and WLN was measured, determining it at pH 6.25 and 8.8, respectively; the MB solution had a pH of 6.85 revealing that the surface of WLW is negatively charged (pHzpc > pH) and MB has a positive charge which favors the electrostatic attraction

towards the adsorption of this dye. Under these conditions the attraction of MO which is an anionic dye that has a negative charge decreases due to the repulsive forces it receives when approaching the surface of WLW because the pH of the solution of this dye is 8.15. In the case of WLN, the opposite occurs since the surface is positively charged at the pH of the MB solution (positive charge), which is repelled by the surface of the adsorbent, decreasing the uptake of the ions of this dye, although under these conditions it favors the adsorption of MO due to having a negative charge, allowing the increase in the removal of this dye in the solution, thereby confirming what was obtained in the kinetics, adsorption isotherm and in the FTIR analysis [Prasad et al., 2021].

CONCLUSIONS

In this study it was shown that *E. crassipes* (WL) with different treatments is a suitable bioadsorbent for the removal of MB and MO present in aqueous solutions at different temperatures, finding that in equilibrium there is adsorption on a heterogeneous surface where there are needed two active sites for each dye molecule. The maximum adsorption capacity obtained in the kinetic study for MB was 200.8 mg/g at 30 °C in WLW and 228.5 mg/g at 60 °C for WLN having a removal percentage up to 92%, while for MO 134.4 mg/g at 30 °C and 155.4 mg/g at 60 °C allowing 80% of this dye to be removed. It was shown that the process is spontaneous with greater randomness in the solid/fluid interface and in the treatment with water it was determined that it is an exothermic process and for WLN it is endothermic. The characterization of these materials indicated that the modification in their surface allows observing that there is a greater crystallinity; moreover, there are functional groups involved in the removal of the dyes together with the participation of electrostatic forces, showing that this material is a good candidate to be used as an adsorbent as it is very cheap, widely available and has great adsorption capacity.

Acknowledgments

REFERENCES

1. Acosta-Rodríguez I., Rodríguez-Pérez A., Pacheco-Castillo N.C., Enríquez-Domínguez E., Cárdenas-González J.F., Martínez-Juárez V.M. 2021. Removal of cobalt (II) from waters contaminated by the biomass of *Eichhornia Crassipes*. Water, 13(13), 1725–1735.

2. Al-Baldawi I.A., Abdullah S.R.S., Almansoory A.F., Ismail N.I., Hasan H.A., Anuar N. 2020. Role of *Salvinia molesta* in biodecolorization of methyl orange dye from water. Sci. Rep., 10, 13980.

3. Alguacil F.J., López F.A. 2021. Organic dyes versus adsorption processing. Molecules, 26(18), 5440–5462.

4. Amalraj R., Ramsenthil R., Durai G., Jayakumar R., Palaniraj R. 2021. Dyes removal using novel sorbents – A review. J. Pharm. Res. Int., 33(45A), 355–382.

5. Anastopoulos I., Hosseini-Bandegharaei A., Fu J., Mitropoulos A.C., Kyzas, G.Z. 2018. Use of nanoparticles to dye adsorption: Review. J. Dispersion Sci. Technol., 39(6), 836–847.

6. Azam K., Raza R., Shezad N., Shabir M., Yang W., Ahmad N., Shafiq I., Akhter A., Hussain M. 2020. Development of recoverable magnetic mesoporous carbon adsorbent for removal of methyl blue and methyl orange from wastewater. J. Environ. Chem. Eng., 8(5), 104220

7. Block I., Günter C. Duarte Rodrigues A., Paasch S., Hesemann P., Taubert A. 2021. Carbon adsorbents from spent coffee for removal of methylene blue and methyl orange from water. Materials, 14(14), 3996–4013.

8. Bożęcka A., Orlof-Naturalna M., Kopeć M. 2021. Methods of dyes removal from aqueous environment. J. Ecol. Eng., 22(9), 111–118.

9. Bronzato G.R.F., Ziegler S.M., Silva R.C., Cesarino I., Leão A.L. 2017. Characterization of the pre-treated biomass of *Eichhornia Crassipes* (water hyacinth) for the second-generation ethanol production, Mol. Cryst. Liq. Cryst., 655(1), 224–235.

10. Deng D., Lamssali M., Aryal N., Ofori-Boadu A., Jha M.K., Samuel R.E. 2020. Textiles wastewater treatment technology: A review. Water Environ. Res., 92, 1805–1810.

11. El-Zawahry M.M., Abdelghaffar F., Abdelghaffar R.A., Mashaly, H.M. 2016. Functionalization of the aquatic weed water hyacinth *Eichhornia Crassipes* by using zinc oxide nanoparticles for removal of organic dyes effluent. Fibers Polym., 17(2), 186–193.

12. Filice S., Bongiorno C., Libertino S., Compagnini G., Gradon L., Iannazzo D., La Magna A., Scalese S. 2021. Structural characterization and adsorption properties of dunino raw halloysite mineral for dye removal from water. Materials, 14(13), 3676–3796.

13. Geed S., Samal K., Tagade A. 2019. Development of adsorption-biodegradation hybrid process for removal of methylene blue from wastewater. J. Environ. Chem. Eng., 7(6), 103439.

14. Giri A.K., Patel R., Mandal S. 2012. Removal of Cr (VI) from aqueous solution biomass-derived by *Eichhornia Crassipes* root activated carbon. Chem. Eng. J., 185–186, 71–81

15. Ghosh G.C., Chakraborty T.K., Zaman S., Nahar M.N., Kabir, A.H.M.E. 2020. Removal of methyl orange dye from aqueous solution by a low cost activated carbon prepared from mahagoni (*Swietenia mahagoni*) Bark. Pollut., 6(1), 171–184.

16. Guan Y., Cao W., Guan H., Lei X., Wang X., Tu Y., Marchetti A., Kong X. (2018). A novel polyalcohol-coated hydroxyapatite for the fast adsorption of organic dyes. Colloids Surf. A., 548, 85–91.

17. Herrera-González A.M., Caldera-Villalobos M., Peláez-Cid A.A. (2019). Adsorption of textile dyes using an activated carbon and crosslinked polyvinyl phosphonic acid composite. J. Environ. Manage., 234, 237–244.

18. Hou Y., Liang Y., Hu H., Tao Y., Zhou J., Cai J. 2021. Facile preparation of multi-porous biochar from lotus biomass for methyl orange removal: Kinetics, isotherms, and regeneration studies. Biores. Technol., 329, 124877.

19. Jedynak K., Repelewicz M., Kurdziel K., Wideł D. 2021. Mesoporous carbons as adsorbents to removal of methyl orange (anionic dye) and methylene blue (cationic dye) from aqueous solutions. Desalin. Water Treat., 220, 363–379.

20. Joaquín-Medina E., Patiño-Saldivar L., Ardila-A.A.N., Salazar-Hernández M., Hernández J.A. 2021. Bioadsorption of methyl orange and methylene blue contained in water using as bioadsorbent Natural Brushite (nDCPD). Tecnología y Ciencias del Agua, 12(3), 304–347.

21. Joudi M., Nasserlah H., Hafdi H., Mouldar J., Hatimi B., El-Mhammedi M.A, Bakasse M. 2020. Synthesis of an efficient hydroxyapatite–chitosan–montmorillonite thin film for the adsorption of anionic and cationic dyes: adsorption isotherm, kinetic and thermodynamic study. SN Appl. Sci., 2, 1078–1091.

22. Kadhom M., Albayati N., Alalwan H., Al-Furaiji M. 2020. Removal of dyes by agricultural waste. Sustainable Chem. Pharm., 16, 100259

23. Kakhki R.M., Rahni S.Y., Karimian A. 2021. Removal of methyl orange from aqueous solutions by a novel, highly efficient and low-cost copper-modified nano-alum. Inorg. Nano-Meter. Chem., 51(9), 1291–1296.

24. Kalam A., Rahman L., Sarker A., Ahmed N., Mustofa M., Awal A. 2021. Efficient removal of toxic textile dye using petiole part (stem) of *Nymphaea alba*. Pollut., 7(3), 643–656.

25. Lacin D., Aroguz A.Z. 2020. Kinetic studies on adsorption behavior of methyl orange using modified halloysite, as an eco-friendly adsorbent. SN Appl. Sci., 2, 2091–2113.

26. Liu Q., Li Y., Chen H., Lu J., Yu G., Möslang M., Zhou Y. 2020. Superior adsorption capacity of

functionalised straw adsorbent for dyes and heavy-metal ions. J. Hazard. Mater., 382, 121040

27. Márquez C.O., García V.J., Guaypatin J.R., Fernández-Martínez F., Ríos A.C. 2021. Cationic and anionic dye adsorption on a natural clayey composite. Appl. Sci., 11(11), 5127–5149.

28. Mishra S., Maiti A. 2017. The efficiency of *Eichhornia Crassipes* in the removal of organic and inorganic pollutants from wastewater: a review. Environ. Sci. Pollut. Res., 24, 7921–7937.

29. Nurhadi M., Widiyowati I.I., Wirhanuddin W., Chandren S. 2019. Kinetic of adsorption process of sulfonated carbon derived from *Eichhornia Crassipes* in the adsorption of methylene blue dye from aqueous solution. Bull. Chem. React. Eng. Catal., 14(1), 17–27.

30. Othman N.H., Alias N.H., Shahruddin M.Z., Abu Bakar N.F., Nik Him N.R., Lau W. J. 2018. Adsorption kinetics of methylene blue dyes onto magnetic graphene oxide. J. Environ. Chem. Eng., 6(2), 2803–2811.

31. Panneerselvam B., Priya K.S. 2021. Phytoremediation potential of water hyacinth in heavy metal removal in chromium and lead contaminated water. Int. J. Environ. Anal. Chem., 4(2), 347–353.

32. Patel S. 2012. Threats, management and envisaged utilizations of aquatic weed *Eichhornia Crassipes*: an overview. Rev. Environ. Sci. Biotechnol., 11, 249–259.

33. Patiño-Saldivar L., Hernández J.A., Ardila A., Salazar-Hernández M., Talavera A., Hernández Soto, R. 2021. Cr (III) removal capacity in aqueous solution in relation to the functional groups present in the orange peel (*Citrus sinensis*). Appl. Sci., 11(14), 6346–6361

34. Prasad R., Sharma D., Yadav K.D., Ibrahim H. 2021. *Eichhornia Crassipes* as biosorbent for industrial wastewater treatment: Equilibrium and kinetic studies. Can. J. Chem. Eng., 100, 439.

35. Priya E.S., Selvan P.S. 2017. Water hyacinth (*Eichhornia Crassipes*) – An efficient and economic adsorbent for textile effluent treatment – A review. Arabian J. Chem., 10, 3548–3558.

36. Rios A.G., Matos L.C., Manrique Y.A., Loureiro J.M., Mendes A., Ferreira A.F.P. 2020. Adsorption of anionic and cationic dyes into shaped MCM-41. Adsorption, 26, 75–88.

37. Rashid N.S.A., Naim M.N., Che Man H., Abu Bakar N.F., Mokhtar M.N. 2019. Evaluation of surface water treated with lotus plant; *Nelumbo nucifera*. J. Environ. Chem. Eng., 7(3), 103048.

38. Rıza Kıvanç M., Ozay O., Ozay H., Ilgin P. 2020. Removal of anionic dyes from aqueous media by using a novel high positively charged hydrogel with high capacity. J. Disper. Sci. Technol., 1000–1015.

39. Saini A., Barman S., Datta D., Sharma K., Kumar K., Goyal N. 2020. Kinetic and thermodynamic study of thionine dye adsorption by peanut hull.

Indian Chem. Eng., 63(5), 522–532.

40. Sharma R., Saini H., Paul D.R., Chaudhary S., Nehra S.P. 2021. Removal of organic dyes from wastewater using *Eichhornia Crassipes*: a potential phytoremediation option. Environ. Sci. Pollut, Res., 28, 7116–7122.

41. Soltani A., Faramarzi M., Parsa S.A.M. 2021. A review on adsorbent parameters for removal of dye products from industrial Wastewater. Water Qual. Res. J., 56(4), 181–193.

42. Srivatsav P., Bhargav B.S., Shanmugasundaram V., Arun J., Gopinath K.P., Bhatnagar A. 2020. Biochar as an eco-friendly and economical adsorbent for the removal of colorants (dyes) from aqueous environment: A review. Water, 12, 3561–3587.

43. Tabinda A.B., Arif R.A., Yasar A., Baquir M., Rasheed R., Ahmood A., Iqbal, A. 2019. Treatment of textile effluents with Pistia stratiotes, *Eichhornia Crassipes* and *Oedogonium* sp. Int. J. Phytorem., 21(10), 939–943.

44. Tara N., Siddiqui S.I., Rathi G., Chaudhry S.A., Inamuddin, Asiri A.M. 2020. Nano-engineered adsorbent for the removal of dyes from water: A review. Curr. Anal. Chem., 16(1), 14–40.

45. Tsade Kara H., Anshebo S.T., Sabir F.K., Workineh G.A. 2021. Removal of methylene blue dye from wastewater using periodiated modified nanocellulose. Int. J. Chem. Eng., 1–16

46. Uddin J., Ampiaw R.E., Lee W. 2021. Adsorptive removal of dyes from wastewater using a metal-organic framework: A review. Chemosphere, 284, 131314.

47. Wanyonyi W.C., Onyari J.M., Shiundu P.M. 2013. Adsorption of methylene blue dye from aqueous solutions using *Eichhornia Crassipes*. Bull. Environ. Contam. Toxicol., 91, 362–366.

48. Xu X., Yu J., Liu C., Yang G., Shi L., Zhuang X. 2021. Xanthated chitosan/cellulose sponges for the efficient removal of anionic and cationic dyes. React. Funct. Polym., 160, 104840.

49. Zaghloul A., Zerbet M., Benhiti R., Abali M., Ichou A.A., Soudani A., Chiban M., Sinan F. 2021. Kinetic, isotherm, and thermodynamic studies of the removal of methyl orange by synthetic clays prepared using urea or coprecipitation. Euro-Mediterranean J. Environ. Integr., 6, 18–27.

50. Zhang B., Wu Y., Cha L. 2019. Removal of methyl orange dye using activated biochar derived from pomelo peel wastes: performance, isotherm, and kinetic studies. J. Dispersion Sci. Technol., 41(1), 125–136.

51. Zhang C., Liu L., Zhao M., Rong H., Xu Y. 2018. The environmental characteristics and applications of biochar. Environ. Sci. Pollut. Res., 25, 21525–21534.

52. Zhu H., Zou H. 2021. Characterization of algae residue biochar and its application in methyl orange wastewater treatment. Water Sci. Technol., 84(12), 3716–3725.